Available online at www.sciencedirect.com
SCIENCE DIRECT®
Chemical Physics Letters 372 (2003) 659–667
CHEMICAL PHYSICS LETTERS
www.elsevier.com/locate/cplett

High-resolution Fourier-transform intra-cavity laser absorption spectroscopy: application to $^{12}C_2H_2$ near 12 300 cm^{-1}

Shui-Ming Hu [a,*], Alain Campargue [b], Zhi-Yong Wu [a], Yun Ding [a,b], An-Wen Liu [a], Qing-Shi Zhu [a]

[a] *Chemical Physics Department, Laboratory of Bond Selective Chemistry, University of Science and Technology of China, Jinzhai Road 96, Hefei 230026, China*

[b] *Laboratoire de Spectrométrie Physique (UMR5588), Université Joseph Fourier de Grenoble, BP 87, 38402 Saint Martin d'Hères, France*

Received 1 February 2003; in final form 14 March 2003

Abstract

The capabilities of intra-cavity laser absorption spectroscopy associated with a high-resolution Fourier-transform spectrometer (FT-ICLAS) are investigated with a Ti:Sapphire laser. Weak absorption lines of atmospheric water were used to test the accuracy of absolute intensity measurements by FT-ICLAS leading to an excellent agreement (a few %) with the HITRAN data. The performances in terms of spectral resolution (0.028 cm^{-1}) and sensitivity (2×10^{-9} cm^{-1}) are illustrated by the spectroscopic study of the overtone spectrum of $^{12}C_2H_2$ between 12 250 and 12 400 cm^{-1} which allowed for a significant improvement of recent cavity ring-down measurements. Among the three Π–Σ bands rotationally analyzed, one is newly observed. The absolute intensity values of the bands are given.

1. Introduction

Among various spectroscopic methods, intra-cavity laser absorption spectroscopy (ICLAS) is characterized by an ultra-sensitivity and a wide field of applications (see [1] for a recent review). The detailed description of ICLAS and references to early papers can be found in [1–3]. The main idea is to place the sample cell inside the cavity of a broad band laser. The resulting spectrum of the sample appears as absorption lines superimposed on the envelope of the broadband laser emission. The equivalent absorption path-length can be evaluated as

$$L_{eq} = c \cdot t_g \cdot l/L, \quad (1)$$

where c is the light speed, t_g is the generation time, and l/L is the ratio of the length of the sample cell with respect to the total length of the laser cavity. As far as the laser spectrum is time resolved, quantitative measurements of extremely weak

* Corresponding author. Fax: +86-551-3602969.
E-mail address: smhu@ustc.edu.cn (S.-M. Hu).

0009-2614/03/$ - see front matter
doi:10.1016/S0009-2614(03)00476-7

transitions can be performed, as demonstrated twenty years ago by Stoeckel et al. [4]. This method was applied in a number of papers (see references in [1]) and gave intensity values which agree with traditional long path cell Fourier-transfer spectroscopy (FTS) measurements when available.

The standard detection scheme in ICLAS uses a grating spectrograph equipped with a charge-coupled-device (CCD) array. The feasibility to associate ICLAS with a Fourier-transform spectrometer (FT-ICLAS) was first demonstrated at medium spectral resolution (0.12 cm^{-1}) by del Olmo et al. [5,6]. We have demonstrated FT-ICLAS experiment at a resolution of 0.05 cm^{-1} [7] with a Ti:Sa laser and a continuous-scan Fourier-transform interferometer which transfer to ICLAS the advantages of the FTS technique: high resolution, low noise, accurate wavenumber calibration and possibility to extend to the infrared region. A similar setup was recently implemented by Hurtmans et al. [8]. However, the possibility to retrieve accurate line intensities from FT-ICLAS spectra based on a continuous-scan FT spectrometer has not been investigated so far. Ideally, the use of a step-scan interferometer as used by Strong et al. [9] and more recently by Guelachivili [10] allows for intensity measurements simular to standard ICLAS [1]. However, a high-spectral resolution with a good sensitivity is difficult to achieve by the step-scan method [10,11]. The aim of the present contribution is to discuss the capability of continuous-scan FT-ICLAS in terms of sensitivity and absolute intensity measurements. The importance to apply an electrical filter to the interference signal in a high-spectral resolution recording will be discussed in the experimental part. The capability to perform microsecond time resolved measurements will also be demonstrated by the measurement of the line intensities of some weak absorption water lines of the atmosphere. Finally as an example of the application of FT-ICLAS, the absorption bands of acetylene near 12 300 cm^{-1} were investigated at Doppler-limited resolution. This region has been recently studied by cavity ring-down spectroscopy (CRDS) and two bands were reported by Metsälä et al. [12]. With the present sensitivity of our FT-ICLAS setup, we could detect one additional band and estimate the band intensities from the absolute intensities of several well-isolated lines.

2. Experimental method of FT-ICLAS

Fig. 1 shows the experimental arrangement. A Bruker IFS 120HR Fourier-transform spectrometer is used to record the interferogram of the laser emission from a home-made 162 cm long standing wave Ti:Sapphire laser. The pumping laser was a Coherent Innova 400 Argon laser which was recently replaced by a Coherent Verdi-5 single mode (532 nm) diode-pumped solid state laser. An 82 cm long sample cell is placed inside the Ti:Sapphire laser cavity. The time sequence of the data acquisition is presented in Fig. 2. A rectangle wave signal, generated by a function generator and synchronized with the sampling pulse of the FT interferometer, was used to drive an acousto-optic modulator (AOM) which chops the pumping laser. The generation time, t_g, is defined as the delay between the sampling pulse of the FT interferometer and the rising edge of the AOM chopping pulse.

The Bruker IFS 120HR interferometer was equipped with a quartz beam-splitter and a Si-diode detector. In FT recording, the spectral wavenumber v is proportional to the frequency f of the electrical signal of the interferogram: $v = v_{\mathrm{He-Ne}} \cdot f/f_{\mathrm{scan}}$, where f_{scan} (in Hz) is the scan velocity of the moving mirror in units of the wavelength of a He–Ne laser, and $v_{\mathrm{He-Ne}} = 15798.021$ cm^{-1} is the wavenumber of the He–Ne laser. Since the spectral width of the ICLAS laser is narrow – typically less than 300 cm^{-1} for a Ti:Sa laser – it corresponds to frequency bandwidth of about 200 Hz at a scan velocity of 10 kHz. The use of a narrow band-pass filter on the signal of interference before the interferogram sampling is then expected to strongly reduce the noise without affecting the spectral region of interest. But it is still questionable as the ICLAS laser is not an ordinary light source: both the absorption lines and the envelope evolve with the generation time [2] and the interference signal is strongly affected by the electrical filtering (see Fig. 2). However, the information of the real

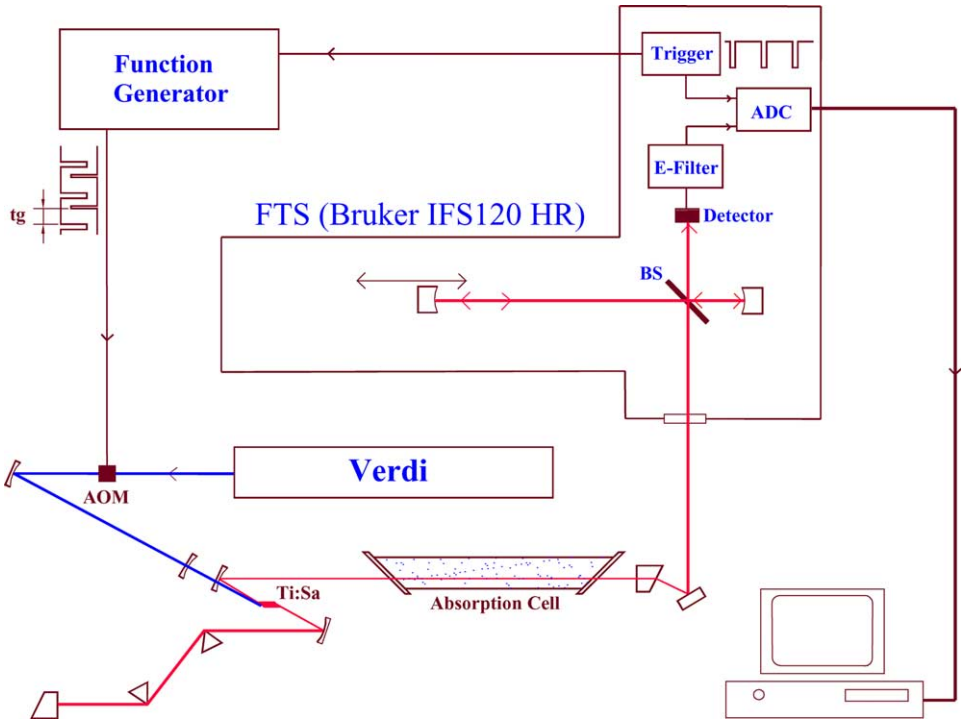

Fig. 1. Configuration of the FT-ICLAS set up. AOM, acousto-optic modulator; BS, beam splitter; ADC, analog-to-digital converter; E-Filter, band-pass electrical filter.

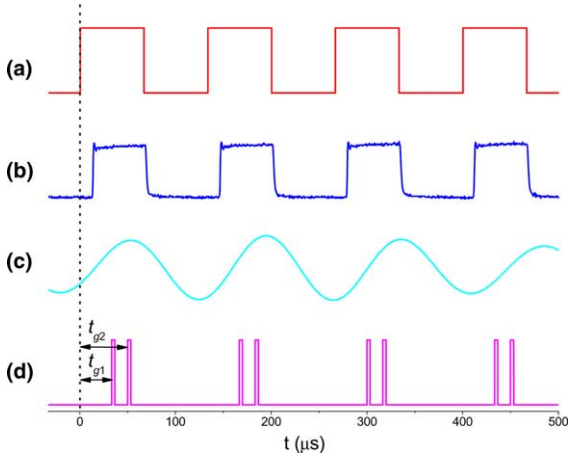

Fig. 2. Interferogram sampling in FT-ICLAS. (a) Rectangle wave which controls the AOM chopping the pumping laser. (b) Interference signal without any electrical filter applied. The data was obtained by detecting the in situ signal of the Si-diode detector with a digital oscilloscope. (c) Interference signal when applied a 5–6 kHz band-pass electrical filter. The data was obtained by detecting the on-board signal after the electrical filter. (d) Sampling signals, two sampling windows at t_{g1} and t_{g2} during the same generation.

spectrum remains: as previously shown in [13], the electrical filter used in FT-ICLAS has no influence on the line positions, but results in a spectrum corresponding to an effective generation time which hinders accurate measurements of absolute line intensities. When the absolute line intensities are measured, electrical filters must be removed and each laser generation must be sampled at identical generation time. Meanwhile, the value of t_g, defined as the delay of the sampling point with the turn-on edge of the AOM driven signal (see Fig. 2), differs from the one defined in Eq. (1) by the build-up time of the laser [14]. So usually, it is necessary to record several (at least two) spectra at different t_g to remove the uncertainty on the time origin. In consequence, the interference signal must be sampled at different generation times within each laser generation (see Fig. 2d). Then, a series of interferogram corresponding to different generation times can be obtained with a time resolution of 1 μs limited by our Si-diode detector. Actually, the interferograms are not sampled

exactly at the same optical path differences contrary to a step-scan system, but this effect can be corrected in the Fourier transformation. Then the real line intensity can be deduced from the series of time-resolved spectra by a linear fitting of the absorbance versus t_g as in standard ICLAS.

Atmospheric absorption by water vapor near 12 600 cm^{-1} was studied to test the accuracy of the line intensity measurement by FT-ICLAS. The spectra were recorded simultaneously at generation times of 30, 40, 50, 60, 70, 80, 90, 100, and 110 μs. A medium resolution of 0.15 cm^{-1} comparable to the width of the air-broadened water lines was adopted for these recordings. The temperature was 300 ± 1 K. The relative humidity was 33% measured by a hygrometer with stated accuracy of ±3%. To retrieve the integrated line intensities of some well-isolated lines, a least square procedure assuming that the line profile results from the convolution of a Voigt function with a Gaussian function corresponding to the apparatus function. The Gaussian component of the Voigt function was fixed to the Doppler profile of water and the baseline was assumed to be a straight line. It is necessary to point out that usually no apodization function should be applied when accurate line positions are concerned, but a strong apodization function, like the Blackman–Harris three term function [15] used here, helps to converge the fitting procedure. The linear dependence of the line intensity value on the generation time is illustrated in Fig. 3. The relative line intensities listed in Table 1 were deduced from the slope of the lines plotted on that figure and agree very well with the HITRAN data [16]. If the molecular density is taken into account at the experiment conditions, the absolute intensities can be calculated (see Table 1). Compared to HITRAN, the systematic deviation of the order of 5% on the absolute intensity values may mainly result from the systematic error on the measured value of the relative humidity.

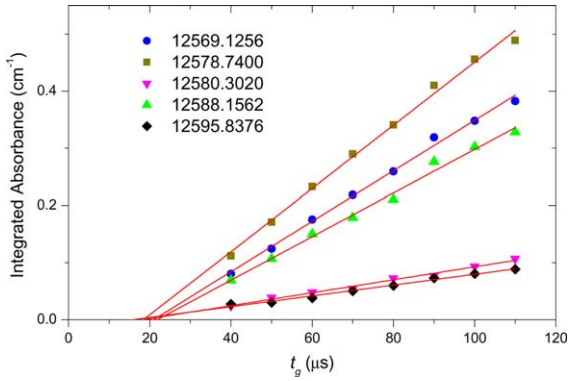

Fig. 3. Variation of the integrated absorbance versus the generation time for different lines of atmospheric water. The line intensities listed in Table 1 were deduced from the slope of the different straight lines by taking into account the concentration of water molecules deduced from the measured humidity rate.

3. Overtone spectroscopy of $^{12}C_2H_2$ near 12 300 cm^{-1}

As an example of the capability of FT-ICLAS in terms of sensitivity and spectral resolution, we investigated the overtone spectrum of $^{12}C_2H_2$ near 12 300 cm^{-1}. The acetylene sample was bought from the Nanking Special Gas Co. with a stated purity of 99.6%. The sample was distilled before

Table 1
Intensities of some water lines obtained from FT-ICLAS spectrum

Position (cm^{-1})	Relative intensity			Absolute intensity		
	HITRAN	ICLAS	δ^b (%)	HITRAN[a]	ICLAS[a]	δ^b (%)
12569.1256	1	1	–	6.36	5.89	−7
12578.7400	1.241	1.254	1	7.89	7.39	−6
12580.3020	0.258	0.258	0	1.64	1.52	−7
12588.1562	0.832	0.864	4	5.29	5.09	−4
12595.8376	0.211	0.215	2	1.34	1.27	−5

[a] Unit: 10^{-25} cm^{-1}/molecule cm^{-2}.
[b] $\delta = \frac{\text{ICLAS–HITRAN}}{\text{HITRAN}}$.

use. The gas pressure was 96.6 hPa measured by a capacitance manometer of 0.5% full-scale accuracy. The frequency of the sampling of the interference was 7.5 kHz which results in a maximum generation time of about 120 μs (corresponding to $l_{eq} = 18$ km). The unapodized resolution was 0.028 cm^{-1}. In order to increase the sensitivity, a 5–6 kHz band-pass electrical filter was applied to improve the signal-noise-ratio (SNR). The corresponding spectrum was used for line positions measurements only. To estimate the line intensities, two additional spectra were recorded without any electrical filter and the interferograms were sampled at two generation times corresponding to 40 and 103 μs. All spectra were recorded at room temperature (297 ± 1 K). For each spectrum, 60 scans were accumulated within 2 h. A comparison of the spectrum obtained with and without electrical filtering shows a gain on the SNR (as light intensity over noise level) of a factor of 3 (see Fig. 4). The sensitivity can be estimated from the absorption coefficient at the noise level $\alpha_{min} \approx (\mathrm{SNR} \cdot ct_g)^{-1}$, with a SNR of about 200, and t_g approximately 100 μs, it leads to a value of 2×10^{-9} cm^{-1}.

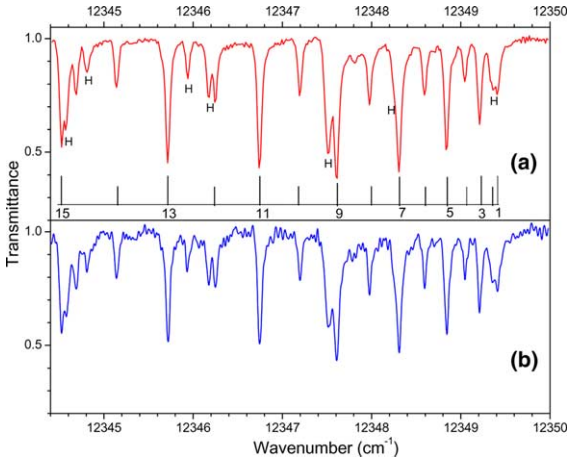

Fig. 4. Comparison of the FT-ICLAS spectrum of $^{12}C_2H_2$ obtained with (a) and without (b) an electric filtering of the interference signal. Note that no apodization was applied here. The spectrum presents the Q branch of the Π_u–Σ_g^+ band at 12349.45 cm^{-1}. The J rotational assignment of the $Q(J)$ lines is given. The $R(17)$–$R(21)$ lines of the Π_u–Σ_g^+ band at 12310.67 cm^{-1} are also observed (but not indicated) on this spectrum. The lines marked by 'H' are residuals due to strong water absorption.

3.1. Rotational analysis

In the studied spectral region, 12 100–12 400 cm^{-1}, three Π_u–Σ_g^+ transitions could be detected. Two of them, were recently reported by Metsälä et al. [12]. After assigning the rotational transitions using the ground state combination differences (GSCD) method, the line positions were fitted on the basis of the standard formula of the energy levels

$$T_v = G_v(v_1, v_2, v_3, v_4^{l_4}, v_5^{l_5}) + F_v(J), \quad (2)$$

where G_v and F_v are the vibrational and rotational contributions, respectively, with $F_v(J) = B_v[J(J+1) - k^2] - D_v[J(J+1) - k^2]^2$, $k = l_4 + l_5$ being the quantum number associated to the total vibrational angular momentum. The rotational l-type doubling contribution to the rotation energy is taken as: $\pm\frac{1}{2}q_vJ(J+1)$, where the + and − signs correspond to the f and e components, respectively. In the fitting procedure, the rotational constants of the ground state, B'' and D'', were constrained to their literature values [17] and the quantities v_0, ΔB, ΔD and q_v were fitted.

The retrieved spectroscopic parameters are gathered in Table 2. In the case of the newly observed transitions at 12288.98 cm^{-1}, the e and f levels of the Π_u upper states could be reproduced in a single simultaneous fit. Similarly to [12], the $\Pi(e)$ and $\Pi(f)$ components of the two other transitions were fitted separately, leading to effective values of the spectroscopic parameters. The comparison with the previous CRDS results, included in Table 2, shows an overall good agreement and a similar quality of the data reproduction (rms of the order of 0.003 cm^{-1}). However, the present observation of weak lines corresponding to higher J values led to a better determination of the parameters, in particular of the distortion constants. In the case of the $\Pi_u(e)$ state at 12310.67 cm^{-1} for instance, our value of the distortion constant differs strongly from the value of [12].

3.2. Vibrational analysis

In these last years, the knowledge of the vibrational energy pattern of $^{12}C_2H_2$ above 10 000

Table 2
Rovibrational parameters (in cm^{-1}) of the Π_u–Σ_g^+ bands of $^{12}C_2H_2$ recorded by ICLAS-FT between 12 100 and 12 400 cm^{-1}

	$(00000)\Sigma_g^{+a}$	G_v 0.0	B_v 1.176 646	$D_v \times 10^6$ 1.627 10				
Band type	v_0[b]	G_v[b]	B_v	$D_v \times 10^6$	$q_v \times 10^3$	J_{MAX} $P/Q/R$	n/N[c]	rms[d]
$\Pi_u(ef)$	12288.9766 (36)	12290.1343 (36)	1.1581911 (47)	−7.60 (27)	5.876 (12)	13/17/11	18/25	3.6
$\Pi_u(e)$	12310.6705 (12)	12311.8223 (12)	1.151816 (17)	0.028 (43)		21/ /15	30/35	3.6
Ref. [12]		12311.8152 (17)	1.151899 (32)	0.37 (12)			/26	3.6
$\Pi_u(f)$	12310.6667 (12)	12311.8231 (12)	1.156359 (12)	1.277 (22)		/27/	21/25	3.1
Ref. [12]		12311.8228 (15)	1.156326 (19)	1.246 (43)			/26	3.5
$\Pi_u(e)$	12349.4501 (12)	12350.6006 (12)	1.150515 (10)	1.649 (18)		20/ /25	30/35	3.6
Ref. [12]		12350.5953 (10)	1.150550 (18)	1.649 (59)			/24	3.6
$\Pi_u(f)$	12349.4493 (22)	12350.6054 (22)	1.1561222 (76)	1.727 (11)		/27/	21/24	2.2
Ref. [12]		12350.6023 (17)	1.156085 (27)	1.616 (74)			/19	3.8

The uncertainties correspond to one standard deviation are listed in parentheses.
[a] The ground state rotational constants are from Kabbadj et al. [17].
[b] The vibrational term value of the upper state is related to the band center: $v_0 = G_v - G_{v''} + B''l''^2 - B'l'^2$.
[c] n, number of transitions included in the fit; N, number of assigned rotational transitions.
[d] Root mean square deviation in $10^{-3}\,cm^{-1}$.

cm^{-1} has been considerably extended in particular by ICLAS (see [18] and references quoted therein). The observed levels were used to refine the vibrational constants of the effective Hamiltonian model [19]. The complete set of predicted vibrational energies and predicted rotational constants B_v for states up to 15 000 cm^{-1} can be found in [20]. The three observed vibrational upper states are univocally assigned to the $\{N_s = v_1 + v_2 + v_3 = 4,\ N_r = 5v_1 + 3v_2 + 5v_3 + v_4 + v_5 = 19,\ k = l_4 + l_5 = 1,\ u\}$ polyad in very good agreement with the predictions from the polyad model, (see Table 3). The vibrational assignment, provided in terms of the dominant zero-order vibrational state in their eigenvector expansion shows, in particular, that the eigenstate of the newly observed level at 12290.13 cm^{-1} is highly mixed as the dominant zero-order

Table 3
Comparison of the experimental and predicted rovibrational parameters of the observed levels of C_2H_2 (in cm^{-1})

Polyad	G_v		B_v		State	Fraction%[c]
	Obs.	Obs.–pred.	Obs.	Pred.		
{4 19 1 u}	12290.13	−0.3	1.1582	1.159	0313^12^0	29
	12311.82	−0.1	1.1541[a]	1.154	1120^01^1	73
	12350.60	0.2	1.1536[b]	1.153	2111^10^0	58
					0131^10^0	28

The calculated values obtained by the effective Hamiltonian model of [19] are tabulated in [20].
[a] Obtained from $(B_e + B_f)/2$.
[b] Dominant zero-order eigenfunctions in the composition of the wavefunction of the observed level, as given by the cluster model [19,20].
[c] Square of the coefficient of the dominant state in the eigenvector expansion. Only states with a fraction higher than 25% are mentioned.

eigenfunctions corresponds to a fraction of only 29%.

3.3. Intensities

The integrated absorbance of several well-isolated rovibrational transitions of the observed bands were deduced from the two spectra corresponding to generation times of 40 and 103 μs, respectively. The method was the same as described in the experimental section, then these values were used to calculate the line strengths. Each line strength S_J (in cm^{-2}/atm at 296 K), corresponding to the transition $\langle v',J'| \leftarrow \langle v,J|$, is related to the modulus square of the transition dipole moment $|R_J|^2$ by the formula [21],

$$S_J = A\frac{\tilde{\nu}C}{QT}g''\exp\left\{-\frac{hcE''}{kT}\right\} \times\left(1-\exp\left\{-\frac{hc\tilde{\nu}}{kT}\right\}\right)|R_J|^2, \quad (3)$$

where A is a constant equal to 3054.72 cm^{-1} atm^{-1} D^{-2}, $\tilde{\nu}$ is the wavenumber of the line, T is the sample temperature in K, E'' and g'' are the energy and degeneracy (including the statistical weight) of the lower level involved in the transition, $C = 0.977828$ is the isotopic abundance of $^{12}C_2H_2$ which is proposed by HITRAN [16], and Q is the total internal partition sum, which can be obtained from [22]. The quantities h, c, and k are Planck's constant, the speed of light, and Boltzman's constant, respectively. If vibration–rotation interaction can be neglected, the modulus square of the transition dipole moment $|R_J|^2$ is usually expressed as $|R_J|^2 = |R_{v'v}|^2 L_J$, where L_J is the Hönl–London factor and $R_{v'v}$ is the vibrational transition moment. For the Π_u–Σ_g^+ transitions discussed here, $L_J = (J-1)/2$, $(2J+1)/2$, and $(J+2)/2$ for P, Q and R branch, respectively [23]. Because only a few lines are well-isolated and involved in the calculation (16 lines altogether), we just give the mean value of $|R_{v'v}|^2$ for the two stronger bands near 12 349 and 12 311 cm^{-1}, which is $0.94(10)\times 10^{-10}$ D^2 and $1.24(31)\times 10^{-10}$ D^2, respectively. The numbers in parentheses represent the statistical uncertainty in the units of the last digits quoted. Because most lines of the weaker band near 12 289 cm^{-1} overlap with strong water lines in this region, it is hard to get accurate absolute line strengths by the same method. However, we estimate that this band is 5–6 times weaker than the band at 12 349 cm^{-1}.

4. Discussion

We have demonstrated the capability of FT-ICLAS to perform accurate quantitative measurement at Doppler resolution. The detection limit of 2×10^{-9} cm^{-1} has allowed for the detection of a new band of $^{12}C_2H_2$ near 12 290 cm^{-1} which could not be observed in a very recent CRDS study performed with a sensitivity of 9×10^{-9} cm^{-1} [12]. The main advantage of FT-ICLAS over conventional ICLAS with grating spectrograph lies in the wide spectral recording and easy accurate wavenumber calibration. For a comparison, the same spectral region of C_2H_2 were also investigated by conventional ICLAS with grating spectrograph equipped with a CCD array in Grenoble (France). As an example, a piece of the spectrum is given in Fig. 5 in the range of the Q branch of the newly detected Π_u–Σ_g^+ band. Conventional ICLAS has the advantage to allow for a more effective correction of the laser baseline than FT-ICLAS. Indeed, atmospheric absorption (mainly water) and different spectral modulations and fringes appear on the laser spectrum. Conventional ICLAS allows for the recording of 15 cm^{-1} wide spectra with and without sample within typically 1 min. The procedure is described in Fig. 5. On this time scale the water concentration and spectral modulations are usually unchanged, leading to a very efficient correction of the background (see Fig. 5). The same procedure can also be applied in FT-ICLAS recording, but more effort is necessary to stabilize the laser during a whole FT recording as the recording time is much longer (typically 1 h), and water concentration can vary in particular as a result of the degasing of the intra-cavity cell. In FT-ICLAS, the spectral stability of the laser over a long time is then a crucial parameter which must be carefully optimized. It is then more difficult to achieve a

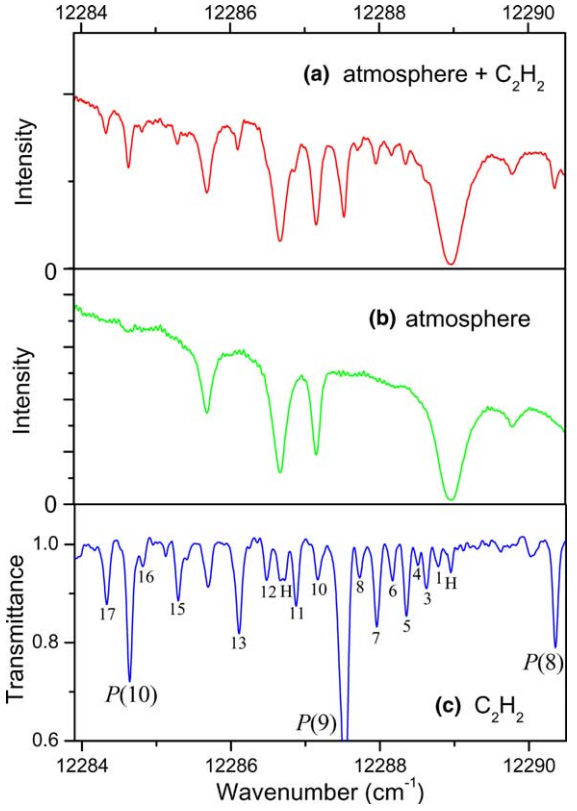

Fig. 5. Illustration of the procedure adopted to remove the atmospheric water contribution in conventional ICLAS experiment with a grating spectrograph. The considered spectral region includes relatively strong absorption of atmospheric water which are easily removed by recording two spectra for the same spectrograph position and for the same generation time (presently $t_g = 310\,\mu s$, $l_{eq} = 45\,km$). The first spectrum (a) is recorded with a given pressure of acetylene (presently 96 hPa) and a second spectrum (b) with the empty cell. The ratio (c) of the first spectrum, thus corresponding to a superposition of C_2H_2 and water absorption contributions, by the second spectrum, due to atmospheric water only, provides the acetylene spectrum. The full procedure is very quick (about 1 min) and then very efficient in conventional ICLAS. The spectrum presents the Q branch of the newly observed Π_u–Σ_g^+ band at $12288.98\,cm^{-1}$ of $^{12}C_2H_2$. The J rotational assignment of the $Q(J)$ lines is given. The stronger $P(10)$–$P(8)$ lines of the Π_u–Σ_g^+ band at $12310.67\,cm^{-1}$ are also rotationally assigned on this spectrum. The lines marked by 'H' are residuals due to strong water absorption.

high sensitivity at high resolution as the recordings require longer accumulation times. Our previous FT-ICLAS study of the absorption spectrum of deuterated water [7] and the present recording of the acetylene spectrum are apparently among the very few studies which could take fully advantage of FTS in term of spectral resolution.

Acknowledgements

This work was jointly supported by the National Natural Science Foundation of China (20103007), National Project for the Development of Key Fundamental Sciences in China, and the Chinese Academy of Science. The support from a collaborative convention between CNRS and CAS (No. 12491) is also acknowledged.

References

[1] M. Herman, J. Liévin, J. Vander Auwera, A. Campargue, Adv. Chem. Phys. 108 (1999) 1.
[2] A. Campargue, F. Stoeckel, M. Chenevier, Spectrochim. Acta Rev. 13 (1990) 69.
[3] A.A. Kachanov, A. Charvat, F. Stoeckel, J. Opt. Soc. Am. B 12 (1995) 970.
[4] F. Stoeckel, M.A. Mélières, M. Chenevier, J. Chem. Phys. 76 (1982) 2191.
[5] A. del Olmo, C. Domingo, J.M. Orza, D. Bermejo, J. Mol. Spectrosc. 145 (1991) 323.
[6] C. Domingo, A. del Olmo, R. Escribano, J.M. Orza, J. Chem. Phys. 96 (1991) 972.
[7] S.-M. Hu, H. Lin, S.-G. He, J.-X. Cheng, Q.-S. Zhu, Phys. Chem. Chem. Phys. 1 (1999) 3727.
[8] D. Hurtmans, S. Kassi, C. Depiesse, M. Herman, Mol. Phys. 100 (2002) 3507.
[9] K. Strong, T. Johnson, G.W. Harris, Appl. Opt. 36 (1997) 8533.
[10] G. Guelachvili, Vib. Spectrosc. 29 (2002) 21.
[11] N. Picqué, G. Guelachivili, Appl. Opt. 39 (2000) 3984.
[12] M. Metsälä, S. Yang, O. Vaittinen, D. Permogorov, L. Halonen, Chem. Phys. Lett. 346 (2001) 373.
[13] J.-X. Cheng, H. Lin, S.-M. Hu, S.-G. He, Q.-S. Zhu, A.A. Kachanov, Appl. Opt. 39 (2000) 2221.
[14] V.M. Baev, T. Latz, P.E. Toschek, Appl. Phys. B 69 (1999) 171.
[15] The function form for the Blackman–Harris three term is $W(\Delta) = a_0 + a_1\cos(2\pi\Delta/\Delta_m) + a_2\cos(4\pi\Delta/\Delta_m)$, where $a_0 = 0.42323$, $a_1 = 0.49755$, and $a_2 = 0.07922$.
[16] L.S. Rothman, C.P. Rinsland, A. Goldman, S.T. Massie, D.P. Edwards, J.M. Flaud, A. Perrin, C. Camy-Peyret, V. Dana, J.Y. Mandin, J. Schrwder, A. McCann, R.R. Gamache, R.B. Wattson, K. Yoshino, K.V. Chance, K.W. Jucks, L.R. Brown, V. Nemtchinov, P. Varanasi, J. Quant. Spectrosc. Radiat. Transfer 60 (1998) 665.
[17] Y. Kabbadj, M. Herman, G. Di Lonardo, L. Fusina, J.W.C. Johns, J. Mol. Spectrosc. 150 (1991) 535.

[18] G. Weirauch, A. Campargue, M.I. El Idrissi, M. Herman, Mol. Phys. 99 (2001) 143.
[19] M.I. El Idrissi, J. Liévin, A. Campargue, M. Herman, J. Chem. Phys. 110 (1999) 2074.
[20] M. Herman, A. Campargue, M.I. El Idrissi, J. Vander Auwera, J. Phys. Chem. Ref. Data (in press).
[21] J. Vander Auwera, J. Mol. Spectrosc. 201 (2000) 143.
[22] R.R. Gamache, R.L. Hawkins, L.S. Rothman, J. Mol. Spectrosc. 142 (1990) 205.
[23] L.S. Rothman, R.L. Hawkins, R.B. Wattson, R.R. Gamache, J. Quant. Spectrosc. Radiat. Transfer 48 (1992) 537.